

# Robust median regression for count data with general truncation: a contaminated discrete Weibull approach

Divan A. Burger<sup>1,2</sup>, Janet van Niekerk<sup>3,4</sup>, Emmanuel Lesaffre<sup>5,6</sup>

<sup>1</sup> *Syneos Health, Bloemfontein, Free State, South Africa*

<sup>2</sup> *Dept. of Mathematical Statistics and Actuarial Science, University of the Free State, Bloemfontein, Free State, South Africa*

<sup>3</sup> *CEMSE Division, King Abdullah University of Science and Technology, Thuwal, Saudi Arabia*

<sup>4</sup> *Dept. of Statistics, University of Pretoria, Pretoria, South Africa*

<sup>5</sup> *I-BioStat, KU Leuven, Leuven, Belgium*

<sup>6</sup> *Department of Statistics and Actuarial Science, University of Stellenbosch, South Africa*

**Abstract:** In right-skewed count data, the mean is disproportionately affected by a long upper tail, whereas the median remains a more representative measure of central tendency. Discrete Weibull (DW) regression links covariates to the log median; however, a single DW component can fit poorly when a small subset of observations is much larger than the remainder of the sample. We propose a contaminated DW (cDW) regression, which augments the baseline DW distribution with a heavier-tailed component while retaining a single shifted-median link. Extreme counts are probabilistically assigned to the heavy-tail component, stabilizing the median-based regression coefficients. The model accommodates general lower truncation at an arbitrary threshold  $c$ , including  $c = 1$  for strictly positive outcomes and  $c = 0$  for nonnegative counts, and is estimated using a straightforward Bayesian Markov chain Monte Carlo algorithm implemented in JAGS; R code accompanies the paper. Applied to hospital length-of-stay data, the cDW regression reduces outlier influence and achieves superior predictive performance relative to a single-component DW model, as demonstrated by leave-one-out cross-validation and a Kullback-Leibler influence diagnostic. Simulation experiments confirm accurate estimation under substantial heavy-tail contamination. Because the added tail component increases probability mass at both extremes, we further recommend embedding the cDW in a hurdle framework when structural zeros are present: the zero probability is modeled separately, and the heavy-tail mixture is applied only to positive counts. The cDW regression model provides a robust, median-centered alternative for analyzing skewed, possibly truncated count outcomes.

**Keywords:** Bayesian inference; count data; heavy tails; median-based regression; mixture models

# 1 Introduction

Count data arise frequently in fields such as epidemiology, healthcare, insurance, and sociology, where the outcome of interest is the number of events or occurrences. A classical modeling choice is the Poisson distribution, but overdispersion, where the variance exceeds the mean, often arises in practice. Many extensions have been proposed to handle overdispersion, including negative binomial (NB) models and zero-inflation/hurdle approaches when there are excess zeros [1].

A separate driver of overdispersion is the presence of outliers or heavy tails, for which standard mean-based approaches (e.g., the NB) may not adequately accommodate extreme observations. In some settings, these heavy tails stem from a subgroup of individuals or entities with far larger counts than the bulk of the population. If left unmodeled, such outliers may disproportionately influence estimates of the mean or regression coefficients, thereby negatively impacting inference and prediction.

Instead of focusing on the mean, which outliers can strongly affect, one can target the median, often a more robust measure of central tendency for skewed or heavy-tailed counts. The discrete Weibull (DW) distribution introduced by Nakagawa & Osaki [2] was extended by Kalktawi [3] and Burger et al. [4] to allow for covariates through a *shifted median*, producing a flexible approach for skewed count data. Still, even a median-based DW can fail to capture extremely large values when a subset of observations exhibits substantially heavier tails than the bulk.

A natural strategy is to adopt a contaminated mixture of distributions, where a fraction of the data follows a heavier-tailed component. This approach is well-established for continuous data, such as contaminated normal distributions [5]. In the count-data setting, robust methods often focus on zero-inflated models, although some researchers have introduced contamination directly into the NB mean regression [6], effectively altering both the left and right tails of the distribution. Indeed, while a heavier right tail is desirable for capturing extreme counts, the mixture can also artificially inflate lower counts, including zeros, that may not truly exist. Such unintended zero inflation complicates model interpretation and parameter estimation. Although not solely for this reason, explicitly mixing a baseline count distribution with a heavier-tailed subcomponent remains relatively uncommon in routine applications.

In this paper, we propose a contaminated DW (cDW) framework that augments the DW distribution of Burger et al. [7] with a heavier-tailed subcomponent and focuses on median regression. We allow for general lower truncation at  $c$ ; in applications, we focus on  $c = 1$  (strictly positive outcomes such as length-of-stay (LOS)), while setting  $c = 0$  recovers the usual (untruncated) DW for nonnegative counts. Our approach extends naturally to regression by linking covariates to the shifted median parameter. A mixture weight  $\delta$  determines how many observations come from the heavier-tailed subcomponent, allowing for more flexible handling of outliers compared to single-component count models.

We first establish the theoretical structure of the truncated DW (TDW) distribution, deriving raw-moment expansions to illustrate its tail limitations. We then introduce the contaminated TDW (cTDW) distribution, which addresses these limitations by adding a heavier-tailed subcomponent, and we demonstrate how to perform Bayesian inference for both regression models. Using a hospital LOS dataset (with no zero-day stays), we show that moderate outliers can noticeably shift parameter estimates in a single-component TDW model, whereas the cTDW model remains more stable and yields improved model adequacy and predictive performance.

Numerous robust methods for outlier-prone count data relate closely to our research, including robust M-estimation in generalized linear models [8] and mixture-based methods that explicitly model outliers [9]. Recent Bayesian frameworks incorporate heavy-tailed priors [10] or simultaneously handle zero inflation and upper-tail outliers in count data [11]. However, many of these remain mean-based. Our framework aims directly at the median count.

NB regression is mean-based, whereas under truncation, the target  $E(Y | Y \geq c)$  couples the mean with  $P(Y < c)$  and lacks a simple one-parameter link. In the cTDW, the shifted-median parameter remains a quantile after truncation, preserving interpretability. A contaminated version of the truncated NB (TNB) would remain mean-centered and, under

truncation, does not admit a simple one-parameter link that preserves the truncated mean; it also has no closed-form median. Accordingly, developing a contaminated TNB (cTNB) is beyond our scope. We include a TNB comparator as a predictive benchmark.

The remainder of this paper is organized as follows. section 2 describes the Arizona LOS dataset that motivates our work. section 3 details the TDW distribution and its contaminated version (cTDW). section 4 explains how we incorporate covariates via a shifted median link. In section 5, we present simulation-based residual diagnostics and Kullback-Leibler (K-L) divergence checks to assess model adequacy and identify outliers, while section 6 describes model comparison via leave-one-out (LOO) cross-validation. section 7 applies the TDW and cTDW models to the hospital LOS data. section 8 reports simulation studies to compare each model’s performance and robustness. Finally, section 9 provides a discussion and outlines a possible hurdle extension, although we do not undertake direct comparisons with other robust count methods here.

## 2 Arizona hospital length-of-stay dataset

Our primary dataset comes from a 1991 Arizona study examining hospital LOS among cardiac patients who underwent one of two revascularization procedures: coronary artery bypass graft (CABG) or percutaneous transluminal coronary angioplasty (PTCA) [12]. CABG bypasses blocked or diseased arteries by grafting new vessels around them, while PTCA uses a balloon to dilate those arteries. Because CABG is typically more invasive, it often leads to longer recovery and thus longer LOS; PTCA is relatively less invasive with shorter recovery [13]. Accordingly, one might expect distinct LOS and risk profiles between these two procedures.

The dataset records total hospital days along with admission type (elective vs. urgent/emergent) and patient sex (male vs. female). Analyzing these variables provides insights into how procedural choice, admission type, and sex influence LOS, which is useful for hospital resource planning and risk management. This dataset was featured by Hilbe [1] in his work on count data regression and is available in the `COUNT` package for R [14].

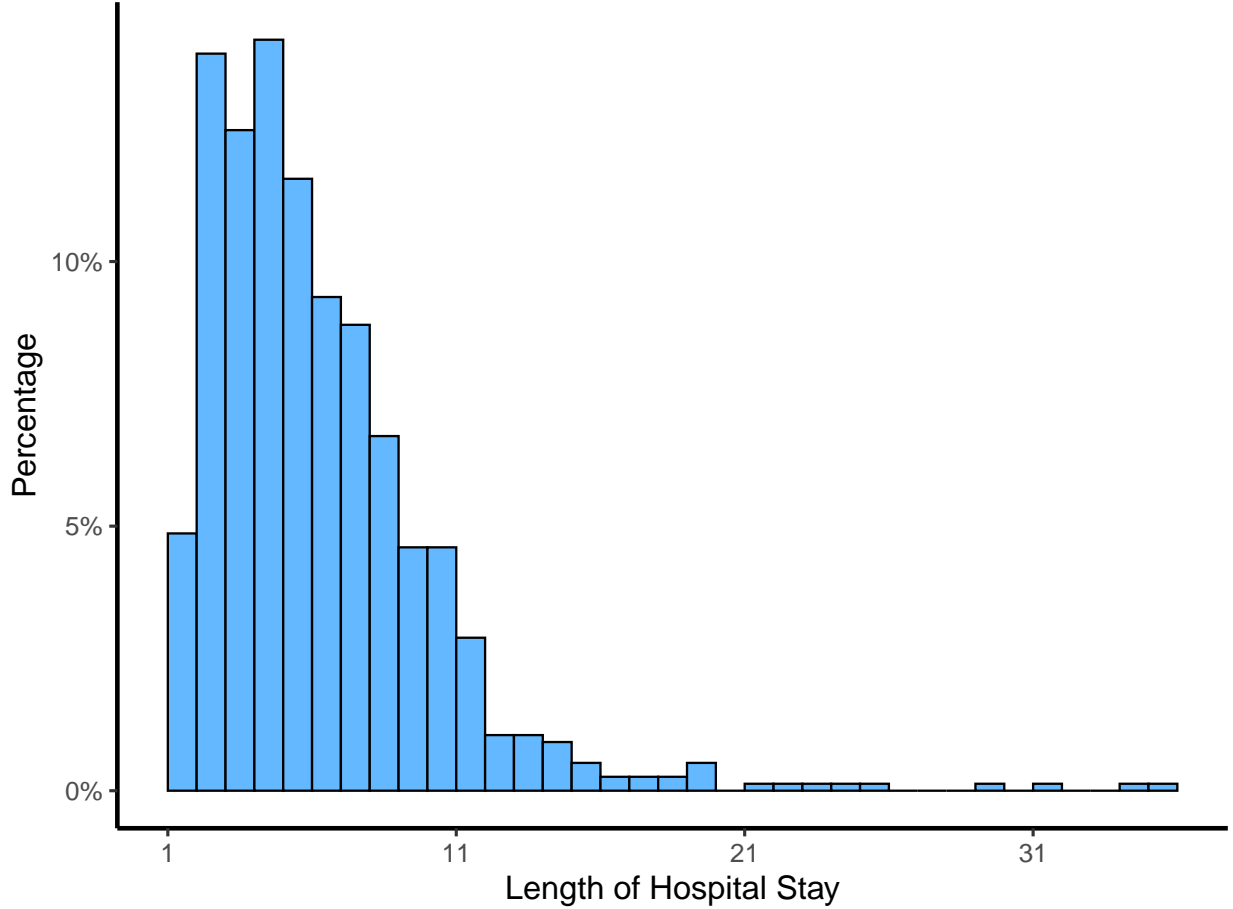
In this dataset, LOS is strictly positive by design. Let  $Y_i$  be the LOS (days) for individual  $i$ ; we therefore model  $Y_i \in \{1, 2, \dots\}$  using the zero-truncated likelihood at  $c = 1$ . This does not assume that  $Y_i = 0$  is possible; it encodes the known lower bound. Recoding  $Z_i = Y_i - 1$  and fitting an untruncated model are not, in general, equivalent. Truncation introduces a parameter-dependent normalizing constant and alters the estimand, except in special cases where the distribution admits a simple shift (e.g., the geometric). Thus, the interpretation of the original LOS scale is preserved only under the truncated specification.

Figure 1 displays the LOS distribution for male patients receiving PTCA on an urgent or emergent basis. The histogram is right-skewed with a pronounced heavy tail: although most stays last only a few days, some extend well beyond two weeks. Such skewness is common in LOS data and calls for models that accommodate heavy tails and outliers.

For context, this Arizona LOS subset has often been analyzed with TNB models in the literature and teaching resources [1, 14, 15]. To mirror that baseline and provide a mean-centered comparator, we also fit a TNB model and report the LOO information criterion (LOOIC). These alternatives target the mean of the untruncated distribution and, under truncation, do not yield a simple regression link to the truncated mean; by contrast, our TDW/cTDW framework links covariates directly to the shifted median, which remains interpretable after truncation and is robust to the heavy upper tail observed in Figure 1.

## 3 Truncated count distributions

We first introduce the TDW distribution (subsection 3.1), describing its probability mass function (PMF) and cumulative distribution function (CDF) and examining its Pearson kurtosis. Analyzing the kurtosis shows that while



**Figure 1:** Distribution of length of hospital stay for male PTCA patients with urgent/emergent admissions.

the single-component TDW distribution is flexible, it may still exhibit limited tail behavior, thereby motivating the mixture approach (cTDW) in subsection 3.2.

### 3.1 Truncated discrete Weibull distribution

For the TDW distribution, we adopt the DW distribution of Nakagawa & Osaki [2], truncating at  $c$  and renormalizing. Based on the standard binomial identity, our moment formulas employ a telescoping approach (see Rosen [16]).

Let  $X$  be a DW random variable on  $\{0, 1, 2, \dots\}$  with parameters  $0 < q < 1$  and  $\rho > 0$ . Its PMF is

$$P_{\text{DW}}(X = n) = q^{n\rho} - q^{(n+1)\rho}, \quad n = 0, 1, 2, \dots$$

Truncating at  $c$  means defining

$$Y = X | (X \geq c),$$

so the total probability from  $n = 0$  to  $n = c - 1$  is removed, and the remainder is renormalized by  $1/q^{c\rho}$ . Thus, the PMF of the TDW distribution can be written as

$$P_{\text{TDW}}(Y = y) = \frac{q^{y\rho} - q^{(y+1)\rho}}{q^{c\rho}}, \quad y = c, c + 1, \dots,$$

and the CDF is

$$F_{\text{TDW}}(y) = 1 - q^{((y+1)^\rho - c^\rho)}, \quad y = c, c+1, \dots$$

The integer median  $m_{\text{med}}$  is the smallest integer  $m$  with  $F(m) \geq 0.5$ . Equivalently,

$$q^{((m+1)^\rho - c^\rho)} \leq 0.5 \iff (m+1)^\rho \geq c^\rho + \frac{\ln(0.5)}{\ln(q)},$$

which leads to

$$m_{\text{med}} = \left\lceil \left( c^\rho + \frac{\ln(0.5)}{\ln(q)} \right)^{\frac{1}{\rho}} - 1 \right\rceil.$$

For simplicity (e.g., in regression modeling), one may drop the ceiling and treat

$$(m+1)^\rho = c^\rho + \frac{\ln(0.5)}{\ln(q)}$$

as a real solution.

To ensure the real median remains above  $c$  (i.e., above the lower bound of the truncated domain), one can define

$$m^* = m + 1 > c, \quad (m^*)^\rho = c^\rho + \frac{\ln(0.5)}{\ln(q)}.$$

Some authors replace  $\rho$  with  $\alpha = 1/\rho$ , so that  $(m^*)^\rho = (m^*)^{1/\alpha}$ . Then

$$(m^*)^{\frac{1}{\alpha}} = c^\rho + \frac{\ln(0.5)}{\ln(q)} \implies q = \exp \left[ \frac{\ln(0.5)}{(m^*)^{\frac{1}{\alpha}} - c^\rho} \right]. \quad (1)$$

Hence, the TDW distribution can equivalently be parameterized by  $(m^*, \alpha)$ , with  $m^* > c$  and  $\alpha > 0$ . Interpreting  $m^*$  as “median + 1” remains convenient, while  $\frac{1}{\alpha}$  controls tail thickness and dispersion: larger  $\alpha$  (i.e., smaller  $\rho$ ) yields heavier right tails and greater dispersion; smaller  $\alpha$  yields lighter tails. This role of the shape parameter is standard for the DW [3] and carries over under truncation. We refer to  $m^*$  as the shifted median and use it as the model’s central tendency measure throughout the paper; it can differ from the exact integer median by no more than a single unit, and in practice the gap is strictly less than one count whenever  $m^*$  is non-integer.

Appendix A details the derivations of the raw moments and Pearson kurtosis for the TDW distribution. Figure 2 plots the kurtosis over various values of  $m^*$  and  $\alpha$  (with  $c = 1$ ), illustrating how the shifted median  $m^*$  and the shape parameter  $\alpha$  govern the distribution’s tail behavior. When  $\alpha = 1$ , the TDW coincides with a truncated geometric distribution on  $\{c, c+1, \dots\}$ ; substituting  $\alpha = 1$  into (A.3) and using (1) (so  $m^* \rightarrow \infty$  implies  $q \rightarrow 1$ ) shows that  $\text{Kurt}(Y) \rightarrow 9$ . If  $\alpha < 1$ , the TDW distribution has lighter tails than this geometric baseline, and the kurtosis converges to a lower plateau (below 9) as  $m^*$  grows. In contrast, if  $\alpha > 1$ , the TDW distribution has heavier tails than the geometric distribution, causing its kurtosis to settle at a higher limiting value (above 9).

### 3.2 Contaminated truncated discrete Weibull distribution

As shown in subsection 3.1, the single-component TDW distribution may not adequately capture heavy-tail behavior or outliers in some applications. To address this, we consider a mixture of two TDW components that share the same shifted median,  $m^*$ , and truncation,  $c$ , but differ in their dispersion parameters. Specifically, let one component have dispersion  $\alpha$ , while the other has dispersion  $\eta\alpha$  with  $\eta > 1$ . We define the cTDW distribution:

$$P_{\text{cTDW}}(Y = y | m^*, \alpha, \eta, \delta, c) = \delta P_{\text{TDW}}(y | m^*, \alpha, c) + (1 - \delta) P_{\text{TDW}}(y | m^*, \eta\alpha, c),$$

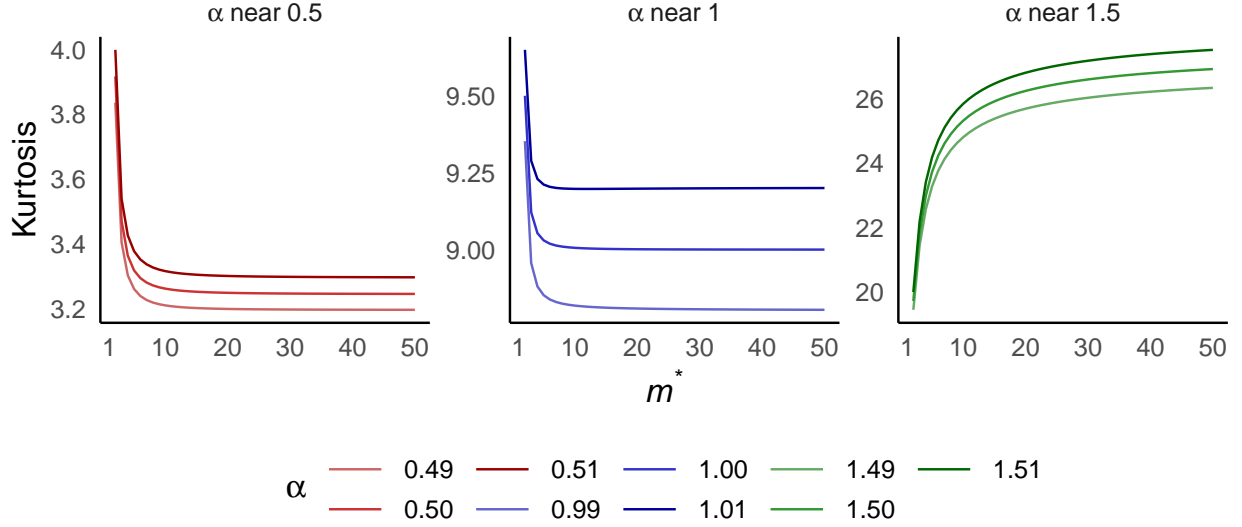


**Figure 2:** Pearson kurtosis of the TDW distribution, plotted against the shifted median  $m^*$ . Each panel shows  $\alpha$  near 0.5, 1, or 1.5 (with slight deviations shown as separate lines). When  $\alpha = 1$ , the TDW distribution coincides with the truncated geometric distribution, whose kurtosis converges to 9. For  $\alpha < 1$ , the TDW distribution has lighter tails than the geometric distribution and settles at a lower plateau. For  $\alpha > 1$ , the TDW distribution has heavier tails, resulting in a higher limiting kurtosis.

for  $y \in \{c, c+1, \dots\}$ , with a minority heavy-tail component enforced by  $\delta \in (0, 0.5)$  and tail inflation  $\eta$ . Hence, with probability  $\delta$ ,  $Y$  is drawn from the narrower TDW  $(m^*, \alpha, c)$ , while with probability  $1 - \delta$ ,  $Y$  comes from the more spread-out TDW  $(m^*, \eta\alpha, c)$ .

Since both sub-distributions share the same pair  $(m^*, c)$ , they also imply the same strict integer median  $m_{\text{med}} = \lceil m^* - 1 \rceil$ . Let  $F_1(y) = F_{\text{TDW}}(y|m^*, \alpha, c)$  and  $F_2(y) = F_{\text{TDW}}(y|m^*, \eta\alpha, c)$  denote the two TDW CDFs. Each satisfies  $F_1(m_{\text{med}}) = F_2(m_{\text{med}}) = 0.5$ . Consequently, the mixture CDF

$$F_{\text{mix}}(y) = \delta F_1(y) + (1 - \delta) F_2(y)$$

inherits  $F_{\text{mix}}(m_{\text{med}}) = 0.5$ . Thus,  $m_{\text{med}}$  remains the overall median of  $Y$  in the cTDW model.

The component with dispersion  $\eta\alpha$  ( $\eta > 1$ ) has heavier tails, inflating the mixture's upper quantiles and allowing better accommodation of extreme counts. In effect, the cTDW captures an excess of large values that a single-component TDW would miss while preserving a common centre and truncation  $c$ .

By centering both mixture components at the same median  $m^*$  and only changing the dispersion parameter ( $\alpha$  vs.  $\eta\alpha$ ), we have a scale mixture, thereby preserving  $m^*$  as the global median. In contrast, a location mixture would allow each sub-distribution its own center, which complicates the determination of a single median.

The two TDW components are distinguishable provided the second component is heavier-tailed, that is, provided  $\eta > 1$ . When  $\eta > 1$ , the right tail of  $P_{\text{TDW}}(y|m^*, \eta\alpha, c)$  decays more slowly than the tail of  $P_{\text{TDW}}(y|m^*, \alpha, c)$ . Because the two PMFs then differ in their tail order, no two distinct parameter triples  $(\alpha, \eta, \delta)$  can produce the same mixture. Hence  $(\alpha, \eta, \delta)$  is identifiable once we impose  $\eta > 1$ . If  $\eta = 1$ , the mixture reduces to a single TDW and the weight  $\delta$  becomes unidentifiable. Throughout the paper, we therefore constrain the prior and the sampler to  $\eta > 1$ , which prevents label switching and ensures a unique set of dispersion parameters.

### 3.3 Truncated negative binomial distribution

For context, we also consider NB models with lower truncation at  $c$  [17]. Let  $X \sim \text{NB}(\mu, \alpha)$  denote the NB distribution parameterized by mean  $\mu > 0$  and dispersion  $\alpha > 0$  (so  $\text{Var}(X) = \mu + \mu^2/\alpha$ ). Let  $P_{\text{NB}}(x|\mu, \alpha)$  and  $F_{\text{NB}}(x|\mu, \alpha)$  denote its PMF and CDF, with  $F_{\text{NB}}(x|\mu, \alpha) = \sum_{k=0}^x P_{\text{NB}}(k|\mu, \alpha)$  for integers  $x \geq 0$ .

Truncating at  $c \in \{1, 2, \dots\}$  means defining

$$Y = X | (X \geq c).$$

Denote the TNB PMF and CDF by  $P_{\text{TNB}}(y|\mu, \alpha, c)$  and  $F_{\text{TNB}}(y|\mu, \alpha, c)$ ; closed forms appear in [Web Appendix A](#) (Supporting Information). The truncated mean is

$$E(Y|\mu, \alpha, c) = \frac{\mu - \sum_{y=0}^{c-1} y P_{\text{NB}}(y|\mu, \alpha)}{1 - F_{\text{NB}}(c-1|\mu, \alpha)}.$$

Therefore,  $E(Y|\mu, \alpha, c)$  depends jointly on  $\mu$  and the lower-tail mass through  $F_{\text{NB}}(c-1|\mu, \alpha)$ . Even with  $\alpha$  and  $c$  fixed, the mapping  $\mu \mapsto E(Y|\mu, \alpha, c)$  is nonlinear and has no closed-form inverse; in particular, one cannot prescribe a target truncated mean and solve algebraically for  $\mu$ . Any such calibration would require numerical root finding. Because this limitation is intrinsic to mean-centered NB models under truncation, a cTNB extension would inherit it and is not pursued here.

## 4 Modeling framework for count data

### 4.1 Regression model specification

Let each observation unit  $i$  have a covariate vector  $\mathbf{x}_i$ , and let  $\boldsymbol{\beta}$  be a regression coefficient vector. We link these covariates to the shifted median  $m_i^*$  by writing

$$\log(m_i^* - c) = \mathbf{x}_i^\top \boldsymbol{\beta}, \quad m_i^* = c + \exp(\mathbf{x}_i^\top \boldsymbol{\beta}), \quad m_i^* > c.$$

Because  $m_i^* - c$  must be strictly positive, the term  $\exp(\mathbf{x}_i^\top \boldsymbol{\beta})$  can span  $(0, \infty)$  for any real-valued  $\mathbf{x}_i^\top \boldsymbol{\beta}$ . This ensures that the median exceeds the truncation point  $c$  neatly.

In the TDW model, the dispersion parameter  $\alpha$  may remain fixed. Each observation  $i$  thus has a TDW PMF,

$$P_{\text{TDW}}(Y_i = y | m_i^*, \alpha, c), \quad y \in \{c, c+1, \dots\}.$$

When heavier tails are suspected, the cTDW model blends two TDW models that share the same median  $m_i^*$  but differ in dispersion  $\alpha$  vs.  $\eta\alpha$  ( $\eta > 1$ ), with a fixed mixing proportion  $\delta$ :

$$P_{\text{cTDW}}(Y_i = y | m_i^*, \alpha, \eta, \delta, c) = \delta P_{\text{TDW}}(y | m_i^*, \alpha, c) + (1 - \delta) P_{\text{TDW}}(y | m_i^*, \eta\alpha, c).$$

Although  $\alpha$ ,  $\delta$ , or  $\eta$  can also depend on covariates (via additional link functions), in this paper, we focus on modeling only  $m_i^*$ .

Further details on model fitting and inference are provided in the next section.

## 4.2 Bayesian inference

In a Bayesian framework, all unknown parameters are treated as random variables. Let

$$\boldsymbol{\theta} = \begin{cases} (\boldsymbol{\beta}, \alpha), & \text{(TDW),} \\ (\boldsymbol{\beta}, \alpha, \eta, \delta), & \text{(cTDW),} \end{cases}$$

where  $\boldsymbol{\beta}$  is the regression coefficients vector,  $\alpha$  the dispersion, and  $\eta > 1$ ,  $\delta$  the additional tail-scaling and mixture parameters (used only in the cTDW counterpart). Given observed data  $\mathcal{D}$ , the posterior distribution of  $\boldsymbol{\theta}$  is defined by

$$p(\boldsymbol{\theta}|\mathcal{D}) \propto L(\mathcal{D}|\boldsymbol{\theta})p(\boldsymbol{\theta}),$$

where  $L(\mathcal{D}|\boldsymbol{\theta})$  is the likelihood for either the TDW or the cTDW model.

We place independent priors on each component of  $\boldsymbol{\theta}$ . Specifically,

$$\begin{aligned} \boldsymbol{\beta} &\sim \mathcal{N}(\mathbf{0}, \sigma_{\beta}^2 \mathbf{I}), & \alpha &\sim \text{Gamma}(a_{\alpha}, b_{\alpha}), \\ \eta &\sim \text{Gamma}(a_{\eta}, b_{\eta})\mathbb{I}_{(1, \infty)}, & \delta &\sim \text{Uniform}(0, 0.5), \end{aligned}$$

where  $\sigma_{\beta}^2$ ,  $(a_{\alpha}, b_{\alpha})$ , and  $(a_{\eta}, b_{\eta})$  are the hyperparameters, and  $\mathbb{I}_{(1, \infty)}$  denotes truncation to  $(1, \infty)$ . One may choose weakly informative priors so that the data primarily drive parameter estimates or more concentrated priors if strong domain knowledge is available. The  $\text{Uniform}(0, 0.5)$  prior on  $\delta$  aligns with the model-level restriction  $\delta \in (0, 0.5)$ , consistent with the robust statistics convention that contamination is a minority phenomenon.

To carry out Bayesian inference, we encode the TDW or cTDW likelihood in JAGS together with the specified priors. Using Markov chain Monte Carlo (MCMC) sampling, JAGS generates samples from the posterior  $p(\boldsymbol{\theta}|\mathcal{D})$ . Once convergence is verified (e.g., via trace plots or the Brooks-Gelman-Rubin potential scale reduction factor (PSRF) [18, 19]), we compute summary statistics such as posterior medians and Bayesian credible intervals (BCIs) directly from the MCMC samples.

## 5 Model adequacy checks

We evaluate model adequacy using the DHARMA package [20], which generates simulation-based quantile residuals from the posterior predictive distribution. Specifically, parameter draws are taken from the fitted posterior, and each draw is used to simulate new responses for every observation. Under correct model specification, these residuals should approximate a  $\text{Uniform}(0, 1)$  distribution. In a uniform quantile-quantile (QQ) plot, the 1:1 diagonal (i.e., the line  $y = x$ ) indicates perfect agreement between the empirical and theoretical quantiles; thus, residuals lying close to this line suggest a well-fitting model.

In addition to the residual checks, we perform a K-L divergence assessment to detect influential observations. Following Wang & Luo [21], we approximate how much the posterior distribution changes when each data point is omitted. Appendix B provides the derivations and the threshold we use for classifying potentially influential observations.

## 6 Model comparison via leave-one-out cross-validation

To compare the predictive performance of different models, we employ LOO cross-validation through the `loo` package [22]. This approach approximates out-of-sample predictive accuracy by using pointwise log-likelihood contributions for each observation evaluated across posterior draws from the full data fit, together with Pareto-smoothed importance sampling (PSIS) to approximate the LOO distribution. Specifically, we extract the log-likelihood for every posterior draw and observation from the full data fit and then apply PSIS to stabilize the estimates of the LOO predictive

densities. The resulting LOOIC and associated metrics (e.g., the effective number of parameters) are used to identify which model provides a better predictive fit. Lower LOOIC values indicate superior generalization to new data.

## 7 Application to hospital length-of-stay data

### 7.1 Implementation and model specification

We apply both the single-component TDW and the cTDW models described in section 4 to the Arizona hospital LOS dataset [1, 14]. Each observation  $i$  has LOS  $Y_i \in \{1, 2, \dots\}$  and covariates: procedure type (CABG or PTCA), admission category (elective or urgent/emergent), and sex (female or male). We encode these as dummy variables in the design matrix  $\mathbf{x}_i$  so that our regression vector  $\boldsymbol{\beta}$  has the following interpretation:

$$\begin{aligned}\beta_0 &= \text{Intercept,} \\ \beta_1 &= \text{CABG vs. PTCA indicator,} \\ \beta_2 &= \text{Urgent/emergent vs. elective indicator,} \\ \beta_3 &= \text{Male vs. female indicator,} \\ \beta_4 &= \text{CABG} \times \text{urgent/emergent interaction,} \\ \beta_5 &= \text{CABG} \times \text{male interaction,} \\ \beta_6 &= \text{Urgent/emergent} \times \text{male interaction,} \\ \beta_7 &= \text{CABG} \times \text{urgent/emergent} \times \text{male (three-way interaction).}\end{aligned}$$

In both the TDW and cTDW fits, we use the shifted-median link:

$$\log(m_i^* - 1) = \mathbf{x}_i^\top \boldsymbol{\beta}, \quad m_i^* > 1.$$

For the TDW model, each observation  $i$  follows

$$P_{\text{TDW}}(Y_i = y | m_i^*, \boldsymbol{\alpha}, c = 1),$$

and for the cTDW model,

$$\begin{aligned}P_{\text{cTDW}}(Y_i = y | m_i^*, \boldsymbol{\alpha}, \boldsymbol{\eta}, \boldsymbol{\delta}, c = 1) &= \delta P_{\text{TDW}}(y | m_i^*, \boldsymbol{\alpha}, c = 1) \\ &+ (1 - \delta) P_{\text{TDW}}(y | m_i^*, \boldsymbol{\eta} \boldsymbol{\alpha}, c = 1),\end{aligned}$$

as described in section 4. Here,  $\boldsymbol{\alpha}$  is the primary dispersion parameter,  $\boldsymbol{\eta} > 1$  scales the heavier-tail component, and  $\boldsymbol{\delta}$  is the mixing proportion. We set  $c = 1$  to reflect the minimum possible hospital stay for this dataset, which is one day.

We assign priors as follows:

$$\begin{aligned}\beta_j &\sim \mathcal{N}(0, 10^3), \quad \boldsymbol{\alpha} \sim \text{Gamma}(0.001, 0.001), \\ \boldsymbol{\eta} &\sim \text{Gamma}(0.001, 0.001) \mathbb{I}_{(1, \infty)}, \quad \boldsymbol{\delta} \sim \text{Uniform}(0, 0.5),\end{aligned}$$

where  $j = 0, 1, \dots, 7$ .

All models are run in JAGS (via the `runjags` package [23]) using four chains, each with 2000 adaptation steps and 4000 burn-in steps. After burn-in, we run each chain for 25 000 iterations, thinning every five draws, which yields 5000 post-burn-in samples per chain. Combining the four chains results in 20 000 total posterior draws for each parameter. Convergence is assessed via the PSRF, which remains at or below 1.05 for all parameters.

We assessed model fit using simulation-based residual diagnostics from the DHARMa package [20] based on 500 posterior predictive draws (see section 5). We compared models using LOO cross-validation in the `loo` package [22] (see

section 6) and identified influential observations by computing the K-L divergence from MCMC-based log-likelihood estimates (also described in section 5).

We fit a TNB model using the same linear predictor and log link as in the DW models, applied to the untruncated NB mean,

$$\log(\mu_i) = \mathbf{x}_i^\top \boldsymbol{\beta}.$$

The dispersion parameter used the same gamma prior as the TDW dispersion. Because the link targets the mean of the untruncated distribution while the data are truncated at  $c$ , there is no simple way to interpret coefficients for the truncated outcome; see [Web Appendix A](#). We therefore report the TNB solely as a predictive benchmark. Posterior sampling and diagnostics followed the same workflow as for the TDW/cTDW fits.

All R code for replicating the results is available on GitHub at [Robust-Count-cTDW](#).

### 7.2 Residual checks and leave-one-out cross-validation

Figure 3 shows the simulation-based residual diagnostics for the TDW and cTDW models. The cTDW residuals align more closely with the uniform diagonal than those from the TDW model. LOO cross-validation likewise favors the cTDW, with  $\text{LOOIC} \approx 19\,583$ , compared with  $\text{LOOIC} \approx 19\,750$  for the TNB, and  $\text{LOOIC} \approx 20\,304$  for the TDW. As the model with the smallest LOOIC is regarded as the preferred one, the cTDW provides the best expected predictive performance. Residual checks for the TNB show departures similar to the TDW (see Supporting Information, [Web Appendix B](#); QQ plot in [Web Figure 1](#)).

### 7.3 Influential observations

Figure 4 presents the K-L divergence plots for the TDW and cTDW models. Fewer observations exceed the K-L threshold for being considered influential under the cTDW model, indicating that the mixture framework better accommodates high-influence data points than the single-component TDW model.

For completeness, [Web Figure 2](#) (Supporting Information, [Web Appendix B](#)) shows that the TNB flags comparatively few influential observations; however, its residual departures resemble those of the TDW, and its predictive fit is intermediate according to LOOIC.

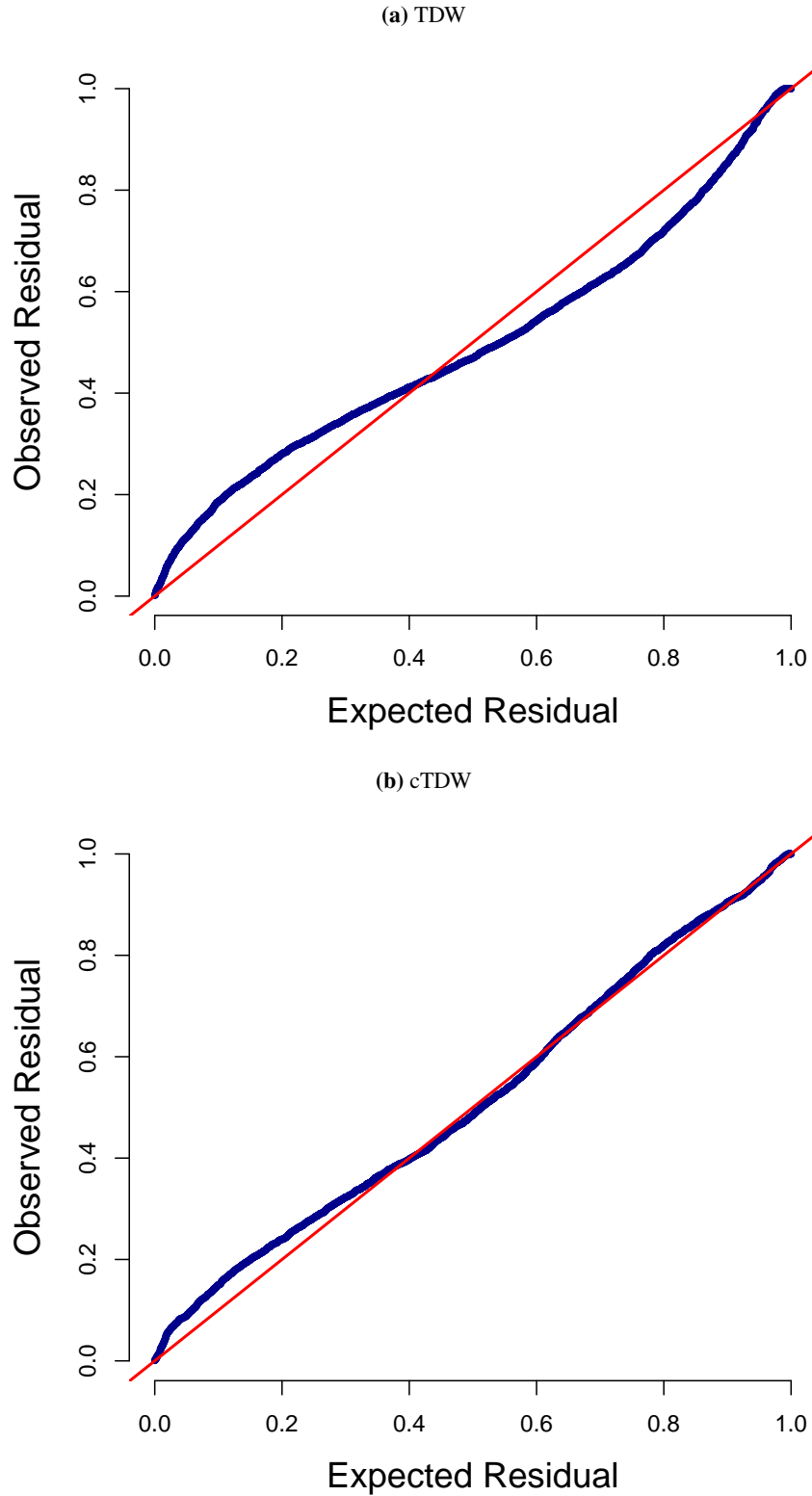
### 7.4 Posterior estimates and median length-of-stay

Figure 5 shows the fitted shifted medians  $m_i^*$  for each subgroup, comparing the single-component TDW and the cTDW models. Overall, the TDW tends to estimate slightly higher medians in some groups, presumably because extreme stays inflate the single-component fit. By contrast, the cTDW accommodates the heavy upper tail in its mixture subcomponent, yielding a slightly lower or tighter center in most subgroups.

Table 2 reports posterior medians and 95% BCIs for  $\{\beta_j\}$ ,  $\alpha$ ,  $\eta$ , and  $\delta$ . The single-component TDW yields  $\alpha \approx 0.58$ , whereas the cTDW shrinks  $\alpha$  to about 0.24 for the narrow subcomponent and inflates the heavy tail with  $\eta \approx 3.1$ . The posterior for the mixture weight concentrates near the upper end of its support ( $\delta \approx 0.50$ ), indicating substantial weight on the clean subcomponent; equivalently, the heavy-tail weight  $1 - \delta$  is at or below one-half.

To assess robustness, we also fit the unrestricted mixture with  $\delta \sim \text{Uniform}(0, 1)$ . Median estimates and 95% BCIs are broadly similar across priors, despite the expected trade-off between the mixture weight  $\delta$  and tail inflation  $\eta$ .

Full sensitivity results appear in the Supporting Information: [Web Figure 3](#) ([Web Appendix B](#)) displays subgroup medians and 95% BCIs under both priors, and [Web Table 1](#) ([Web Appendix C](#)) reports the corresponding parameter summaries.



**Figure 3:** QQ plots of simulation-based residuals for (a) the single-component TDW model and (b) the cTDW model. The blue points show the empirical distribution of residuals against the ideal uniform distribution (red diagonal). Compared to the single-component TDW model, the cTDW residuals adhere more closely to the diagonal, indicating improved model fit.

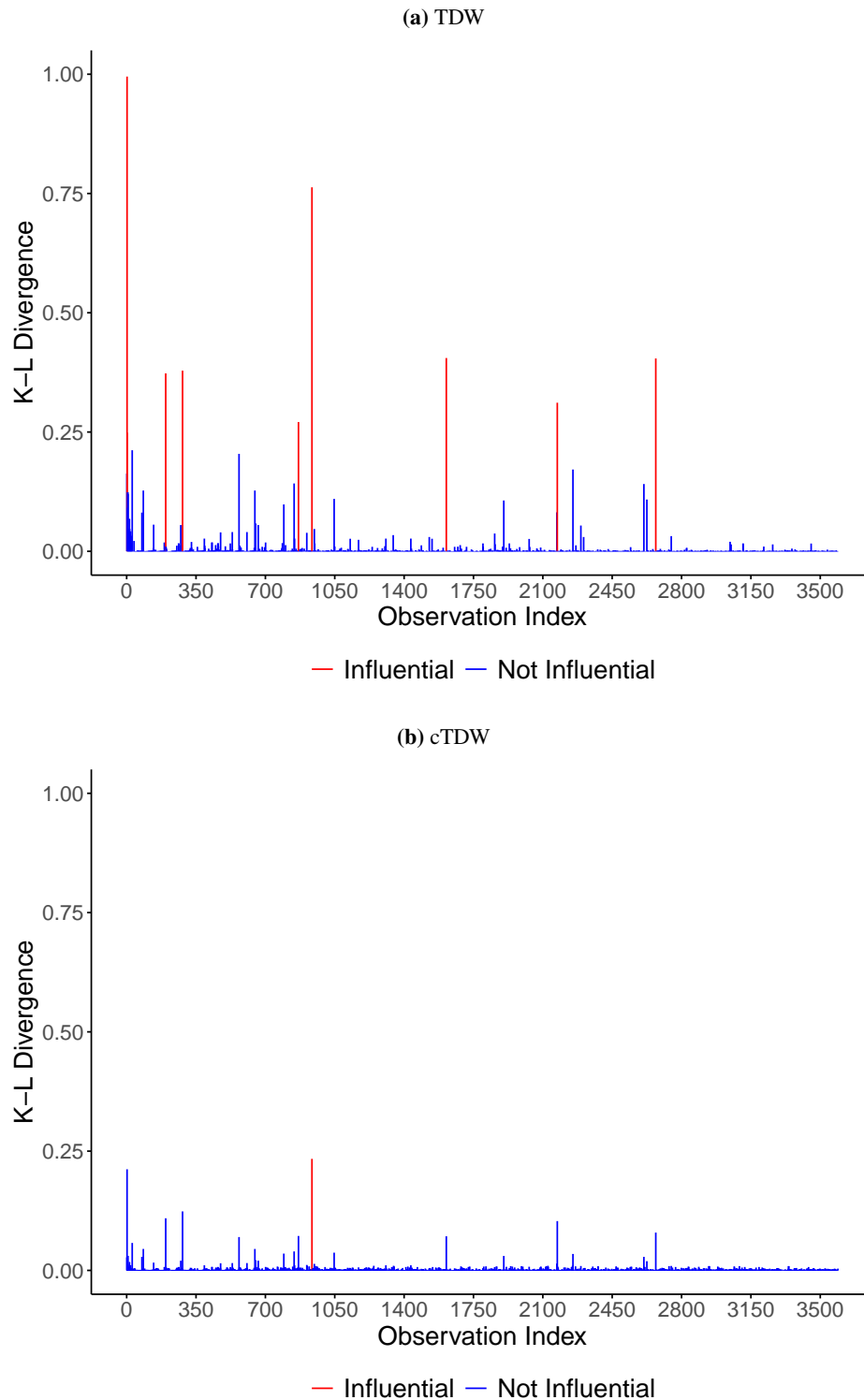


**Figure 4:** K-L divergence plots for (a) the TDW and (b) the cTDW models. Each vertical bar represents an observation, colored red if classified as influential and blue otherwise. Under the single-component TDW model, several points exhibit disproportionately large influence, whereas the cTDW mixture reduces these outliers by better accommodating heavy-tailed behavior.

**Table 2:** Posterior medians (Est.) and 95% BCIs for the single-component TDW and cTDW models applied to the Arizona hospital LOS data. The regression coefficients  $\beta_j$  link covariates to a shifted median via  $\log(m_i^* - 1) = \mathbf{x}_i^\top \boldsymbol{\beta}$ , where  $\beta_1$  through  $\beta_7$  capture the effects of procedure type (CABG vs. PTCA), admission category (urgent/emergent vs. elective), and sex (male vs. female), including interactions. The dispersion parameter is  $\alpha$  in both models, whereas  $\eta$  and  $\delta$  appear only in the cTDW model to inflate the heavier-tail subdistribution and determine its mixing proportion, respectively.

Parameter	Model					
	TDW			cTDW		
	Est.	95% BCI		Est.	95% BCI	
$\beta_0$	1.023	[ 0.926;	1.117]	0.844	[ 0.759;	0.934]
$\beta_1$	1.283	[ 1.152;	1.418]	1.461	[ 1.350;	1.563]
$\beta_2$	0.722	[ 0.613;	0.836]	0.865	[ 0.757;	0.965]
$\beta_3$	-0.106	[-0.221;	0.015]	-0.073	[-0.183;	0.030]
$\beta_4$	-0.457	[-0.619;	-0.300]	-0.621	[-0.747;	-0.482]
$\beta_5$	-0.005	[-0.166;	0.151]	-0.056	[-0.180;	0.078]
$\beta_6$	-0.072	[-0.213;	0.066]	-0.082	[-0.207;	0.055]
$\beta_7$	0.046	[-0.146;	0.243]	0.083	[-0.091;	0.240]
$\alpha$	0.584	[ 0.569;	0.599]	0.244	[ 0.230;	0.260]
$\eta$				3.111	[ 2.893;	3.343]
$\delta$				0.497	[ 0.485;	0.500]

## 8 Simulation study

To investigate the performance of the proposed cTDW model and compare it against the single-component TDW model, we conducted a simulation study involving data contamination scenarios. Specifically, we considered a single-covariate regression setting of the form

$$\log(m_i^* - c) = \beta_0 + \beta_1 x_i,$$

where  $m_i^*$  denotes the shifted median for observation  $i$ ,  $c$  is the lower bound, and  $\beta_0$  and  $\beta_1$  are regression coefficients. In each replicate of the simulation, we generated response counts  $Y_i$  from the cTDW model with parameters  $\{\beta_0, \beta_1, \alpha, \eta, \delta\}$  and a fixed sample size  $N$ . We then fitted both the single-component TDW and cTDW models to each generated dataset to quantify the effects of contamination on estimation accuracy.

For each lower bound setting  $c \in \{0, 1\}$ , for each sample size  $N \in \{50, 100, 200\}$ , and for each contamination setting  $(\eta, \delta) \in \{(2, 0.10), (2, 0.45), (5, 0.45)\}$ , we generated 1000 independent datasets. We specified true values  $\beta_0 = 2$ ,  $\beta_1 = 0.3$ , and  $\alpha = 0.6$ . In total, we considered 18 scenarios, arising from three sample sizes, two truncation limits, and three contamination settings ( $3 \times 2 \times 3 = 18$ ).

We used the `autorun.jags` feature of the `runjags` package [23] to ensure full convergence across all simulation replicates.

We derived the following performance metrics for each parameter across the 1000 replicates: mean bias, root mean squared error (RMSE), coverage probability (CP) of the 95% BCIs, and the average 95% BCI length. These summaries appear in Table 3 and Table 4.

Table 3 reports the mean bias and CPs for all parameters under the cTDW model. Across most scenarios, coverage probabilities remain close to or above the nominal level, suggesting generally adequate (and occasionally conservative) inference. However, the  $\eta$  parameter often exhibits noticeable bias under lighter contamination, which is a typical penalty when the data do not fully support a heavier-tail structure.

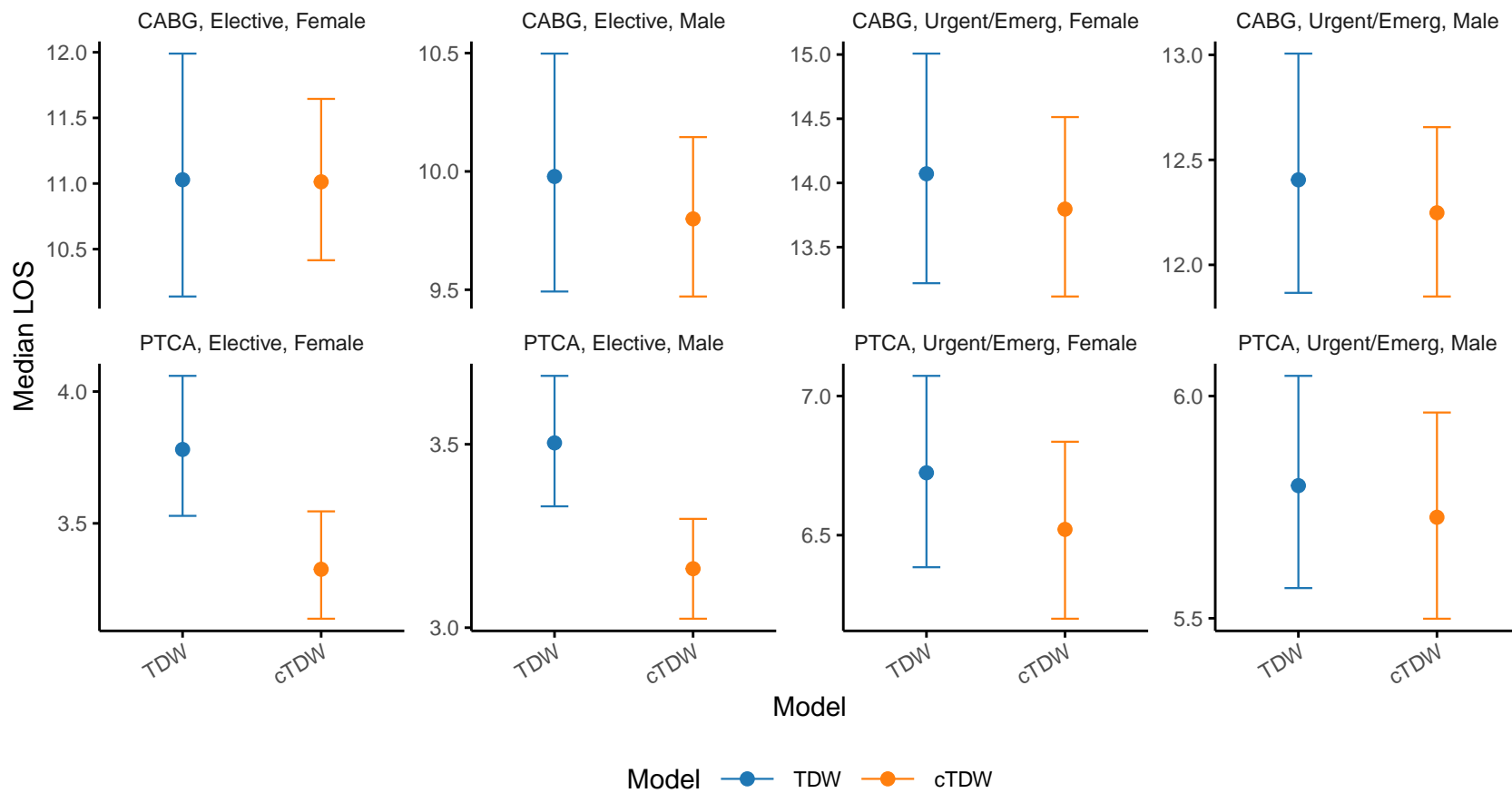


**Figure 5:** Posterior estimates of the shifted median  $m^*$  for each subgroup, modeled under the single-component TDW and cTDW models. Each point represents the posterior median of  $m^*$ , and the vertical bars (whiskers) show the corresponding 95% BCI. Facets distinguish the combinations of procedure type, admission category, and patient sex. The TDW estimates (blue) and cTDW estimates (orange) are displayed side by side for each subgroup.

**Table 3** contrasts the simulation metrics for the regression coefficients  $\beta_0$  and  $\beta_1$  between the TDW and cTDW models. Both models perform similarly when contamination is mild ( $\eta = 2, \delta = 0.1$ ). However, under heavier contamination ( $\eta = 5, \delta = 0.45$  or  $\eta = 10, \delta = 0.45$ ), the TDW model exhibits inflated RMSE and wider BCIs across both  $c = 0$  and  $c = 1$ . In particular, the coverage for  $\beta_1$  drops markedly when  $c = 0$ , whereas the cTDW model remains comparatively robust.

**Table 3:** Simulation results for the cTDW model under various contamination settings. For each combination of  $c, \eta, \delta$ , and sample size  $N$ , 1000 datasets were generated. The table shows each parameter’s mean bias and the 95% BCI CP.

$\eta$	$\delta$	$N$	Parameter	Value	$c = 0$		$c = 1$	
					Bias	CP	Bias	CP
2	0.1	50	$\beta_0$	2.00	-0.0058	0.937	-0.0128	0.946
			$\beta_1$	0.30	0.0018	0.942	-0.0042	0.954
			$\alpha$	0.60	-0.2379	0.993	-0.2208	0.991
			$\eta$	2.00	3.4418	0.993	4.4482	0.985
			$\delta$	0.10	0.0422	0.997	0.0470	0.999
2	0.1	100	$\beta_0$	2.00	-0.0001	0.938	-0.0066	0.945
			$\beta_1$	0.30	0.0060	0.943	-0.0008	0.953
			$\alpha$	0.60	-0.1277	0.996	-0.1328	0.993
			$\eta$	2.00	2.2689	0.992	2.2870	0.987
			$\delta$	0.10	0.0342	0.997	0.0385	0.999
2	0.1	200	$\beta_0$	2.00	-0.0042	0.932	-0.0020	0.954
			$\beta_1$	0.30	-0.0002	0.947	0.0002	0.950
			$\alpha$	0.60	-0.0534	0.985	-0.0441	0.993
			$\eta$	2.00	1.9058	0.982	1.5131	0.991
			$\delta$	0.10	0.0261	0.997	0.0358	1.000
5	0.45	50	$\beta_0$	2.00	0.0158	0.949	-0.0167	0.937
			$\beta_1$	0.30	0.0065	0.941	0.0094	0.939
			$\alpha$	0.60	-0.0988	0.952	-0.1244	0.971
			$\eta$	5.00	1.8735	0.967	5.3175	0.966
			$\delta$	0.45	-0.1069	0.971	-0.1580	0.980
5	0.45	100	$\beta_0$	2.00	0.0139	0.938	-0.0069	0.947
			$\beta_1$	0.30	0.0047	0.954	0.0024	0.940
			$\alpha$	0.60	-0.0393	0.963	-0.0729	0.966
			$\eta$	5.00	0.4517	0.965	1.6805	0.959
			$\delta$	0.45	-0.0504	0.984	-0.1094	0.971
5	0.45	200	$\beta_0$	2.00	0.0116	0.945	-0.0002	0.947
			$\beta_1$	0.30	0.0016	0.957	0.0019	0.941
			$\alpha$	0.60	-0.0209	0.948	-0.0369	0.965
			$\eta$	5.00	0.2334	0.951	0.5434	0.964
			$\delta$	0.45	-0.0278	0.977	-0.0592	0.970
10	0.45	50	$\beta_0$	2.00	0.0034	0.957	-0.0231	0.937
			$\beta_1$	0.30	0.0039	0.963	-0.0063	0.939
			$\alpha$	0.60	-0.0202	0.976	0.0255	0.970
			$\eta$	10.00	1.2956	0.976	15.6141	0.946
			$\delta$	0.45	-0.0542	0.981	-0.1271	0.989

Continued on next page

**Table 3 – continued from previous page**

$\eta$	$\delta$	$N$	Parameter	Value	$c = 0$		$c = 1$	
					Bias	CP	Bias	CP
10	0.45	100	$\beta_0$	2.00	0.0100	0.944	0.0012	0.959
			$\beta_1$	0.30	-0.0044	0.958	0.0025	0.953
			$\alpha$	0.60	-0.0089	0.959	-0.0410	0.971
			$\eta$	10.00	0.4601	0.950	6.1765	0.947
			$\delta$	0.45	-0.0277	0.978	-0.0748	0.971
10	0.45	200	$\beta_0$	2.00	0.0046	0.950	0.0069	0.953
			$\beta_1$	0.30	0.0004	0.955	0.0071	0.946
			$\alpha$	0.60	-0.0081	0.962	-0.0270	0.951
			$\eta$	10.00	0.2731	0.949	1.6156	0.946
			$\delta$	0.45	-0.0161	0.980	-0.0411	0.975

## 9 Discussion

In this paper, we introduce a cDW framework for modeling robust count data. Building on the TDW distribution, we introduce a heavier-tailed subcomponent that absorbs outliers while preserving a single median parameter  $m^*$ . Applying the cTDW model to Arizona hospital length-of-stay data (truncated at  $c = 1$ ) reveals marked improvements in residual diagnostics and predictive accuracy (via LOO cross-validation) compared with the single-component TDW model, particularly in capturing extreme hospital stays. Moreover, K-L divergence checks show that the cTDW approach flags far fewer high-influence points than the TDW model, indicating its capacity to handle outliers effectively.

For completeness, we fit a TNB solely as a predictive benchmark. Its predictive performance was intermediate (worse than cTDW, better than TDW); the K-L divergence profile was considerably milder than TDW, but the residual QQ plot still showed departures from uniformity. Given the lack of a clear coefficient interpretation under truncation, we did not interpret the TNB parameters.

Our simulation study compared the cTDW model with a single-component TDW model under mild and heavy contamination scenarios, varying sample sizes, and lower bounds. The cTDW model consistently maintained nominal coverage levels, even in the presence of outliers, whereas the TDW model suffered from inflated RMSE, wider BCIs, and lower coverage under heavier contamination. These findings suggest that a heavier-tail subcomponent can substantially improve performance in the presence of outliers.

Although we focus on  $c = 1$  for strictly positive data (as in the length of stay), setting  $c = 0$  allows the cTDW model to cover the full range  $\{0, 1, 2, \dots\}$ . A heavier-tailed component, however, increases mass at both extremes. When genuinely large values drive overdispersion but the data do not contain extra zeros, this left-tail behavior can spuriously inflate the fitted probability at  $Y = 0$ . The same issue is known for heavy-tailed Poisson mixtures [24], such as the generalized gamma or Sichel models. A practical remedy is to separate the zero cell from the positive counts by embedding the cTDW in a hurdle or zero-inflated framework: the hurdle models  $P(Y = 0)$  directly, while the heavy-tail mixture is applied only to  $Y \in \{1, 2, \dots\}$ . Concretely, one may define

$$P(Y = y) = \begin{cases} \pi, & y = 0, \\ (1 - \pi) P_{\text{cTDW}}(Y = y | m^*, \alpha, \eta, \delta, c = 1), & y \in \{1, 2, \dots\}, \end{cases}$$

thereby avoiding over-predicting zeros or misrepresenting heavy right tails among the positive counts.

Overall, our results suggest that the cTDW model provides a flexible and robust framework for analyzing count data with outliers, particularly when the median is the preferred measure of location and a heavier-tailed subpopulation is

**Table 4:** Simulation results for the TDW and cTDW models across all scenarios. For each combination of  $c$ ,  $\eta$ ,  $\delta$ , and sample size  $N$ , 1000 datasets were generated. The table presents the fixed effects' mean bias, RMSE, 95% BCI CP, and the average 95% BCI length.

$c$	$\eta$	$\delta$	$N$	Parameter	Value	Model							
						TDW				cTDW			
						Bias	RMSE	CP	BCI lgth	Bias	RMSE	CP	BCI lgth
0	2	0.1	50	$\beta_0$	2.00	-0.0028	0.2007	0.947	0.7857	-0.0058	0.2100	0.937	0.7552
				$\beta_1$	0.30	0.0003	0.1773	0.938	0.6848	0.0018	0.1812	0.942	0.6955
0	2	0.1	100	$\beta_0$	2.00	0.0000	0.1366	0.958	0.5515	-0.0001	0.1418	0.938	0.5347
				$\beta_1$	0.30	0.0029	0.1265	0.942	0.4746	0.0060	0.1298	0.943	0.4805
0	2	0.1	200	$\beta_0$	2.00	-0.0018	0.0998	0.945	0.3858	-0.0042	0.1024	0.932	0.3747
				$\beta_1$	0.30	-0.0011	0.0853	0.945	0.3276	-0.0002	0.0859	0.947	0.3314
0	5	0.45	50	$\beta_0$	2.00	0.0531	0.3430	0.961	1.5491	0.0158	0.2298	0.949	0.9052
				$\beta_1$	0.30	0.0073	0.4177	0.882	1.3474	0.0065	0.2564	0.941	0.9340
0	5	0.45	100	$\beta_0$	2.00	0.0551	0.2395	0.978	1.0922	0.0139	0.1469	0.938	0.5769
				$\beta_1$	0.30	-0.0018	0.2851	0.888	0.9296	0.0047	0.1362	0.954	0.5490
0	5	0.45	200	$\beta_0$	2.00	0.0549	0.1769	0.968	0.7719	0.0116	0.0991	0.945	0.3914
				$\beta_1$	0.30	0.0003	0.2093	0.861	0.6543	0.0016	0.0904	0.957	0.3592
0	10	0.45	50	$\beta_0$	2.00	0.2456	0.6656	0.983	3.0770	0.0034	0.2171	0.957	0.9391
				$\beta_1$	0.30	0.0050	0.8157	0.900	2.6704	0.0039	0.2405	0.963	0.9728
0	10	0.45	100	$\beta_0$	2.00	0.2359	0.5109	0.962	2.1564	0.0100	0.1436	0.944	0.5730
				$\beta_1$	0.30	-0.0015	0.5789	0.882	1.8289	-0.0044	0.1347	0.958	0.5268
0	10	0.45	200	$\beta_0$	2.00	0.2024	0.3684	0.966	1.5279	0.0046	0.0975	0.950	0.3862
				$\beta_1$	0.30	-0.0054	0.4035	0.880	1.2807	0.0004	0.0845	0.955	0.3378
1	2	0.1	50	$\beta_0$	2.00	-0.0117	0.1899	0.956	0.7678	-0.0128	0.1984	0.946	0.7360
				$\beta_1$	0.30	-0.0028	0.1654	0.956	0.6561	-0.0042	0.1731	0.954	0.6650
1	2	0.1	100	$\beta_0$	2.00	-0.0088	0.1293	0.958	0.5361	-0.0066	0.1320	0.945	0.5172
				$\beta_1$	0.30	-0.0001	0.1152	0.947	0.4452	-0.0008	0.1162	0.953	0.4493
1	2	0.1	200	$\beta_0$	2.00	-0.0048	0.0918	0.964	0.3779	-0.0020	0.0935	0.954	0.3662
				$\beta_1$	0.30	0.0014	0.0795	0.949	0.3137	0.0002	0.0812	0.950	0.3166
1	5	0.45	50	$\beta_0$	2.00	-0.0606	0.2349	0.974	1.0302	-0.0167	0.2145	0.937	0.8319
				$\beta_1$	0.30	0.0142	0.2377	0.937	0.8846	0.0094	0.2095	0.939	0.7884
1	5	0.45	100	$\beta_0$	2.00	-0.0729	0.1750	0.959	0.7320	-0.0069	0.1442	0.947	0.5641
				$\beta_1$	0.30	0.0082	0.1710	0.925	0.6153	0.0024	0.1387	0.940	0.5247

Continued on next page

Table 4 – continued from previous page

<i>c</i>	$\eta$	$\delta$	<i>N</i>	Parameter	Value	Model							
						TDW				cTDW			
						Bias	RMSE	CP	BCI lgth	Bias	RMSE	CP	BCI lgth
1	5	0.45	200	$\beta_0$	2.00	-0.0811	0.1378	0.942	0.5164	-0.0002	0.0964	0.947	0.3838
				$\beta_1$	0.30	0.0084	0.1204	0.924	0.4321	0.0019	0.0938	0.941	0.3542
1	10	0.45	50	$\beta_0$	2.00	-0.1033	0.2935	0.961	1.2281	-0.0231	0.2431	0.937	0.9120
				$\beta_1$	0.30	-0.0087	0.2829	0.933	1.0669	-0.0063	0.2252	0.939	0.8737
1	10	0.45	100	$\beta_0$	2.00	-0.1179	0.2215	0.953	0.8715	0.0012	0.1499	0.959	0.5956
				$\beta_1$	0.30	0.0020	0.1985	0.935	0.7365	0.0025	0.1414	0.953	0.5603
1	10	0.45	200	$\beta_0$	2.00	-0.1344	0.1881	0.899	0.6112	0.0069	0.1036	0.953	0.4025
				$\beta_1$	0.30	0.0060	0.1390	0.925	0.5123	0.0071	0.0948	0.946	0.3658

present. The contaminated structure provides a practical alternative to standard overdispersed or zero-inflated models in settings where extremely large counts drive the overdispersion.

## Research ethics

Not applicable.

## Author contributions

All authors have accepted responsibility for the entire content of this manuscript and approved its submission.

## Competing interests

The authors state no competing interests.

## Research funding

This work is based on the research supported by the National Research Foundation (NRF) of South Africa (Grant number 132383). Opinions expressed and conclusions arrived at are those of the authors and are not necessarily to be attributed to the NRF.

## Data availability statement

The Arizona hospital LOS dataset used in this article is freely available from the COUNT package in R. All R code for reproducing the application results can be found on GitHub at Robust-Count-cTDW.

## Appendix A Truncated discrete Weibull kurtosis

The  $k^{\text{th}}$  raw moment of the TDW random variable  $Y$ , taking values in  $\{c, c+1, \dots\}$ , is given by

$$\mathbb{E}(Y^k) = \sum_{y=c}^{\infty} y^k P_{\text{TDW}}(Y=y) = \frac{1}{q^{c^p}} \sum_{y=c}^{\infty} y^k (q^{y^p} - q^{(y+1)^p}). \quad (\text{A.1})$$

We use the binomial identity

$$n^k - (n-1)^k = \sum_{j=0}^{k-1} \binom{k}{j} (-1)^{(k-1-j)} n^j.$$

which implies

$$n^k = \sum_{m=1}^n (m^k - (m-1)^k).$$

Hence, each  $y^k$  in (A.1) can be expanded as

$$y^k = \sum_{m=1}^y (m^k - (m-1)^k).$$

Substituting into (A.1) and applying Tonelli's Theorem [25] (i.e., interchanging sums of nonnegative terms) gives

$$\mathbb{E}(Y^k) = \frac{1}{q^{c\rho}} \sum_{y=c}^{\infty} \left[ \sum_{m=1}^y (m^k - (m-1)^k) \right] (q^{y\rho} - q^{(y+1)\rho}).$$

Rearranging, we get

$$\mathbb{E}(Y^k) = \frac{1}{q^{c\rho}} \sum_{m=1}^{\infty} (m^k - (m-1)^k) \sum_{y=\max(c,m)}^{\infty} (q^{y\rho} - q^{(y+1)\rho}).$$

Observe that if  $m < c$ , the inner sum starts at  $y = c$ ; if  $m \geq c$ , it starts at  $y = m$ . After telescoping,

$$\sum_{y=m}^{\infty} (q^{y\rho} - q^{(y+1)\rho}) = q^{m\rho}, \quad \sum_{y=c}^{\infty} (q^{y\rho} - q^{(y+1)\rho}) = q^{c\rho}.$$

Here, we use the fact that  $0 < q < 1$  and  $\rho > 0$ , so  $q^{(N+1)\rho} \rightarrow 0$  as  $N \rightarrow \infty$ , causing the upper boundary terms to vanish in the telescoping sum.

Combining these yields

$$\mathbb{E}(Y^k) = (c-1)^k + \frac{1}{q^{c\rho}} \sum_{m=c}^{\infty} (m^k - (m-1)^k) q^{m\rho}. \quad (\text{A.2})$$

The term  $(c-1)^k$  arises from summing over  $m = 1, \dots, c-1$ .

If  $c = 1$ , then  $(c-1)^k = 0$  and  $q^{c\rho} = q$ . Thus, (A.2) reduces to the simpler

$$\mathbb{E}(Y^k) = \frac{1}{q} \sum_{m=1}^{\infty} (m^k - (m-1)^k) q^{m\rho}.$$

With  $\mathbb{E}(Y^k)$  for  $k = 1, 2, 3, 4$  in hand, the variance is

$$\sigma^2 = \mathbb{E}(Y^2) - \mu^2, \quad \text{where } \mu = \mathbb{E}(Y).$$

The fourth central moment is

$$\mathbb{E}\left((Y - \mu)^4\right) = \mathbb{E}(Y^4) - 4\mu\mathbb{E}(Y^3) + 6\mu^2\mathbb{E}(Y^2) - 4\mu^3\mathbb{E}(Y) + \mu^4.$$

The Pearson kurtosis is

$$\text{Kurt}(Y) = \frac{\mathbb{E}\left((Y - \mu)^4\right)}{(\text{Var}(Y))^2}. \quad (\text{A.3})$$

Hence, by plugging in the series expansions for  $\mathbb{E}(Y^k)$ , one can compute the kurtosis numerically and study its limiting behavior under varying  $\rho$ ,  $q$ , or (equivalently)  $\alpha$ ,  $m^*$ .

## Appendix B Kullback-Leibler divergence for outlier detection

To assess the influence of each individual observation on the TDW or cTDW fit, we adopt a LOO approach similar to the methodology of Wang and Luo [21]. Specifically, we evaluate the K-L divergence between the posterior distributions obtained with and without a given observation. Large K-L values indicate that omitting a certain data point meaningfully shifts the posterior, suggesting that the point may be an outlier.

Denote by  $\boldsymbol{\theta}^{(k)}$  the  $k^{\text{th}}$  posterior draw of these parameters, for  $k = 1, \dots, K$ . Suppose the dataset  $\mathcal{D}$  contains observations  $\mathcal{D}_i$ . We write  $P(\boldsymbol{\theta} | \mathcal{D})$  for the posterior given the full dataset and  $P(\boldsymbol{\theta} | \mathcal{D}_{[i]})$  for the posterior distribution when observation  $\mathcal{D}_i$  is removed. Following Wang & Luo [21], the K-L divergence between these two posteriors under

model  $R$  (TDW or cTDW) is approximated as:

$$\text{KL}_R(P(\boldsymbol{\theta}|\mathcal{D}), P(\boldsymbol{\theta}|\mathcal{D}_{[i]})) = \log \left\{ \frac{1}{K} \sum_{k=1}^K [P(\mathcal{D}_i|\boldsymbol{\theta}^{(k)})]^{-1} \right\} + \frac{1}{K} \sum_{k=1}^K \log [P(\mathcal{D}_i|\boldsymbol{\theta}^{(k)})]. \quad (\text{B.4})$$

In (B.4), each  $P(\mathcal{D}_i|\boldsymbol{\theta}^{(k)})$  corresponds to the model likelihood (TDW or cTDW) evaluated at the posterior draw  $\boldsymbol{\theta}^{(k)}$ . A higher  $\text{KL}_R$  value indicates that removing  $\mathcal{D}_i$  significantly alters the posterior, implying that the point may be influential or an outlier under model  $R$ .

We follow Tomazella et al. [26] in labeling an observation  $\mathcal{D}_i$  as an outlier if:

$$0.5 \left( 1 + \sqrt{1 - \exp[-2\text{KL}_R(P(\boldsymbol{\theta}|\mathcal{D}), P(\boldsymbol{\theta}|\mathcal{D}_{[i]}))]} \right) \geq 0.8. \quad (\text{B.5})$$

This criterion flags data points that significantly alter the posterior distribution when omitted, indicating an unusually large influence on parameter estimates. In practice,  $\text{KL}_R$  is computed for each  $\mathcal{D}_i$ , and (B.5) is applied to identify points that have a disproportionate impact on the posterior.

## References

- [1] Hilbe JM. Negative Binomial Regression. Cambridge University Press; 2011.
- [2] Nakagawa T, Osaki S. The discrete Weibull distribution. IEEE Transactions on Reliability. 1975;24(5):300-1.
- [3] Kalktawi HS. Discrete Weibull Regression Model for Count Data [Ph.D. thesis]. Brunel University London; 2017.
- [4] Burger DA, Schall R, Ferreira JT, Chen DG. A robust Bayesian mixed effects approach for zero inflated and highly skewed longitudinal count data emanating from the zero inflated discrete Weibull distribution. Statistics in Medicine. 2020;39(9):1275-91.
- [5] Hampel FR, Ronchetti EM, Rousseeuw PJ, Stahel WA. Robust Statistics: The Approach Based on Influence Functions. Wiley Series in Probability and Statistics. John Wiley & Sons; 2011.
- [6] Otto AF, Ferreira JT, Tomarchio SD, Bekker A, Punzo A. A contaminated regression model for count health data. Statistical Methods in Medical Research. 2025;34(2):369-89.
- [7] Burger DA, Lesaffre E. Nonlinear mixed-effects modeling of longitudinal count data: Bayesian inference about median counts based on the marginal zero-inflated discrete Weibull distribution. Statistics in Medicine. 2021;40(23):5078-95.
- [8] Cantoni E, Ronchetti E. Robust inference for generalized linear models. Journal of the American Statistical Association. 2001;96(455):1022-30.
- [9] Beath KJ. A mixture-based approach to robust analysis of generalised linear models. Journal of Applied Statistics. 2018;45(12):2256-68.
- [10] Datta J, Dunson DB. Bayesian inference on quasi-sparse count data. Biometrika. 2016;103(4):971-83.
- [11] Hamura Y, Irie K, Sugawara S. Robust Bayesian modeling of counts with zero inflation and outliers: theoretical robustness and efficient computation. Journal of the American Statistical Association. 2025;0(0):0-0.
- [12] National Health Economics & Research Co . 1991 Arizona Medpar data, cardiovascular patient files; 1991. Arizona, U.S.
- [13] Fihn SD, Gardin JM, Abrams J, Berra K, Blankenship JC, Dallas AP, et al. 2012 ACCF/AHA/ACP/AATS/PCNA/SCAI/STS guideline for the diagnosis and management of patients with

- stable ischemic heart disease: executive summary: a report of the American College of Cardiology Foundation/American Heart Association Task Force on Practice Guidelines, and the American College of Physicians, American Association for Thoracic Surgery, Preventive Cardiovascular Nurses Association, Society for Cardiovascular Angiography and Interventions, and Society of Thoracic Surgeons. *Journal of the American College of Cardiology*. 2012;60(24):2564-603.
- [14] Hilbe JM, Robinson R. COUNT: functions, data and code for count data; 2025. R package version 1.3.4. Available from: <https://CRAN.R-project.org/package=COUNT>.
- [15] Hardin JW, Hilbe JM. Regression models for count data from truncated distributions. *The Stata Journal*. 2015;15(1):226-46.
- [16] Rosen KH. *Discrete Mathematics and Its Applications*. 8th ed. New York, NY, USA: McGraw-Hill Education; 2019.
- [17] Sampford MR. The truncated negative binomial distribution. *Biometrika*. 1955;42(1-2):58-69.
- [18] Gelman A, Rubin DB. Inference from iterative simulation using multiple sequences. *Statistical Science*. 1992;7(4):457-72.
- [19] Brooks SP, Gelman A. General methods for monitoring convergence of iterative simulations. *Journal of Computational and Graphical Statistics*. 1998;7(4):434-55.
- [20] Hartig F, Lohse L, de Souza M. DHARMA: residual diagnostics for hierarchical (multi-level / mixed) regression models; 2024. R package version 0.4.7. Available from: <https://cran.r-project.org/web/packages/DHARMA/index.html>.
- [21] Wang J, Luo S. Augmented Beta rectangular regression models: A Bayesian perspective. *Biometrical Journal*. 2016;58(1):206-21.
- [22] Vehtari A, Gabry J, Magnusson M, Yao Y, Bürkner PC, Paananen T, et al.. loo: efficient leave-one-out cross-validation and WAIC for Bayesian models; 2024. R package version 2.8.0. Available from: <https://cran.r-project.org/web/packages/loo/index.html>.
- [23] Denwood MJ. runjags: An R package providing interface utilities, model templates, parallel computing methods and additional distributions for MCMC models in JAGS. *Journal of Statistical Software*. 2016;71(9):1-25.
- [24] Karlis D, Xekalaki E. Mixed Poisson distributions. *International Statistical Review*. 2005;73(1):35-58.
- [25] Folland GB. *Real Analysis: Modern Techniques and Their Applications*. John Wiley & Sons; 1999.
- [26] Tomazella VLD, Jesus S, Gazon AB, Louzada F, Nadarajah S, Nascimento DC, et al. Bayesian reference analysis for the generalized normal linear regression model. *Symmetry*. 2021;13(5):856.

## Supporting information

Additional supporting information can be found online.

# **Robust median regression for count data with general truncation: a contaminated discrete Weibull approach**

Divan A. Burger, Janet van Niekerk, and Emmanuel Lesaffre

## **Supporting Information**

## Web Appendix A. Truncated negative binomial distribution

Let  $X \sim \text{NB}(\mu, \alpha)$  with mean  $\mu > 0$  and dispersion  $\alpha > 0$ . Its PMF is

$$P_{\text{NB}}(x|\mu, \alpha) = \frac{\Gamma(x + \alpha)}{\Gamma(\alpha)\Gamma(x + 1)} \left(\frac{\alpha}{\alpha + \mu}\right)^\alpha \left(\frac{\mu}{\alpha + \mu}\right)^x, \quad x \in \{0, 1, 2, \dots\}.$$

Let  $F_{\text{NB}}(x|\mu, \alpha) = \sum_{k=0}^x P_{\text{NB}}(k|\mu, \alpha)$  denote its CDF.

Truncating at  $c \in \{1, 2, \dots\}$  means defining

$$Y = X | (X \geq c).$$

The TNB PMF and CDF are

$$P_{\text{TNB}}(Y = y|\mu, \alpha, c) = \frac{P_{\text{NB}}(y|\mu, \alpha)}{1 - F_{\text{NB}}(c - 1|\mu, \alpha)}, \quad y \in \{c, c + 1, \dots\},$$

$$F_{\text{TNB}}(y|\mu, \alpha, c) = \frac{F_{\text{NB}}(y|\mu, \alpha) - F_{\text{NB}}(c - 1|\mu, \alpha)}{1 - F_{\text{NB}}(c - 1|\mu, \alpha)}, \quad y \geq c.$$

For  $c \in \{1, 2, \dots\}$ , the truncated mean is

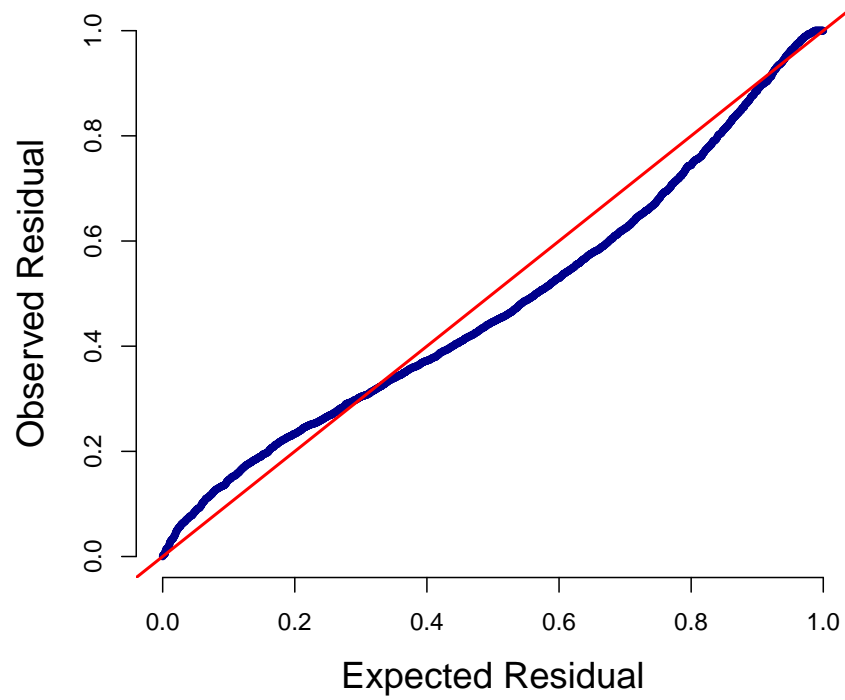
$$E(Y|\mu, \alpha, c) = E(X|X \geq c) = \frac{\mu - \sum_{y=0}^{c-1} y P_{\text{NB}}(y|\mu, \alpha)}{1 - F_{\text{NB}}(c - 1|\mu, \alpha)}.$$

Substituting the NB PMF gives an explicit form for the lower-tail first moment:

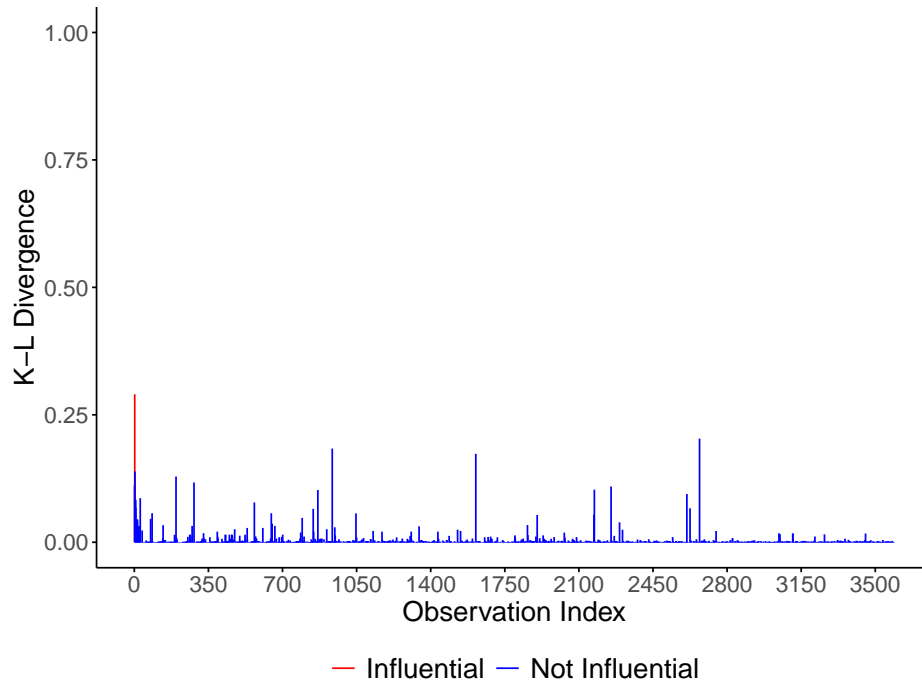
$$\sum_{y=0}^{c-1} y P_{\text{NB}}(y|\mu, \alpha) = \sum_{y=1}^{c-1} y \frac{\Gamma(y + \alpha)}{\Gamma(\alpha)\Gamma(y + 1)} \left(\frac{\alpha}{\alpha + \mu}\right)^\alpha \left(\frac{\mu}{\alpha + \mu}\right)^y,$$

and, using  $y\Gamma(y + \alpha)/\Gamma(y + 1) = \Gamma(y + \alpha)/\Gamma(y)$ ,

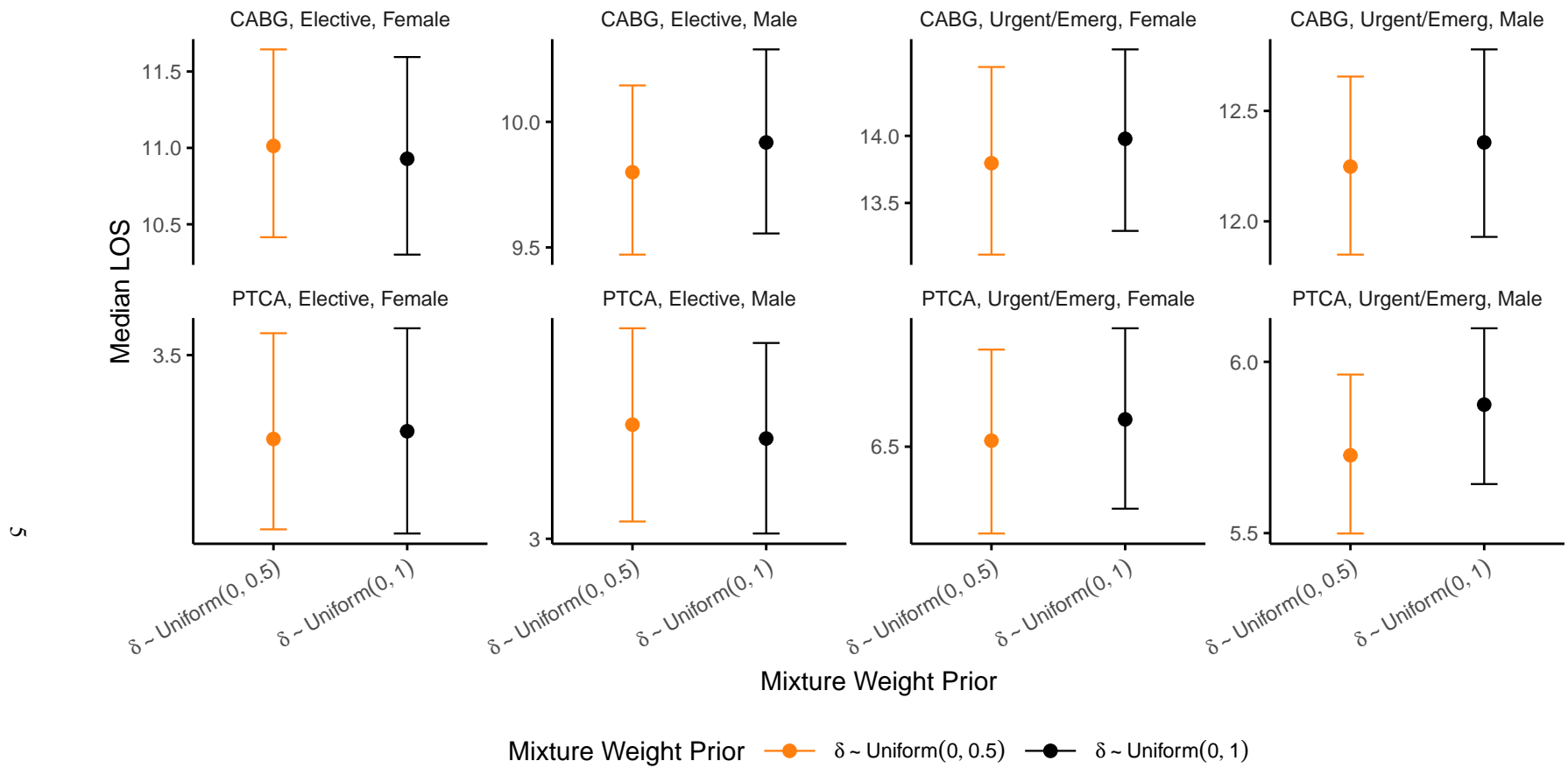
$$\sum_{y=0}^{c-1} y P_{\text{NB}}(y|\mu, \alpha) = \left(\frac{\alpha}{\alpha + \mu}\right)^\alpha \left(\frac{\mu}{\alpha + \mu}\right) \sum_{k=0}^{c-2} \frac{\Gamma(k + \alpha + 1)}{\Gamma(\alpha)\Gamma(k + 1)} \left(\frac{\mu}{\alpha + \mu}\right)^k.$$

**Web Appendix B. Figures**

**Web Figure 1:** QQ plot of simulation-based residuals for the TNB model. The blue points show the empirical distribution of residuals against the ideal uniform distribution (red diagonal). Departures from the diagonal mirror those under the single-component TDW, indicating a comparable lack of fit.



**Web Figure 2:** K-L divergence plot for the TNB model. Each vertical bar represents an observation, colored red if classified as influential and blue otherwise. Relative to the single-component TDW, the TNB shows fewer and smaller influential points, indicating a more stable influence profile.



**Web Figure 3:** Posterior estimates of the shifted median  $m^*$  for each subgroup under the cTDW model with two mixture weight priors. Each point is the posterior median of  $m^*$ , and the vertical bars show the 95% BCI. Facets distinguish the combinations of procedure type, admission category, and patient sex. Orange corresponds to  $\delta \sim \text{Uniform}(0, 0.5)$  (contamination restriction) and black to  $\delta \sim \text{Uniform}(0, 1)$  (sensitivity). Median estimates and 95% BCIs are similar across priors.

## Web Appendix C. Tables

**Web Table 1:** Posterior medians (Est.) and 95% BCIs for the cTDW model applied to the Arizona hospital LOS data under two prior specifications for the mixing proportion  $\delta$ . The regression coefficients  $\beta_j$  link covariates to a shifted median via  $\log(m_i^* - 1) = \mathbf{x}_i^\top \boldsymbol{\beta}$ , where  $\beta_1$  through  $\beta_7$  capture the effects of procedure type (CABG vs. PTCA), admission category (urgent/emergent vs. elective), and sex (male vs. female), including interactions. The dispersion parameter is  $\alpha$ , while  $\eta$  and  $\delta$  inflate the heavier-tail subdistribution and determine its mixing proportion, respectively. Results are shown for  $\delta \sim \text{Uniform}(0, 0.5)$  (model-level contamination restriction) and for  $\delta \sim \text{Uniform}(0, 1)$  (sensitivity analysis allowing a more flexible mixture).

Parameter	cTDW Model			
	$\delta \sim \text{Uniform}(0, 0.5)$		$\delta \sim \text{Uniform}(0, 1)$	
	Est.	95% BCI	Est.	95% BCI
$\beta_0$	0.844	[ 0.759; 0.934]	0.851	[ 0.761; 0.944]
$\beta_1$	1.461	[ 1.350; 1.563]	1.445	[ 1.332; 1.555]
$\beta_2$	0.865	[ 0.757; 0.965]	0.871	[ 0.765; 0.978]
$\beta_3$	-0.073	[-0.183; 0.030]	-0.089	[-0.202; 0.019]
$\beta_4$	-0.621	[-0.747; -0.482]	-0.603	[-0.738; -0.466]
$\beta_5$	-0.056	[-0.180; 0.078]	-0.019	[-0.151; 0.118]
$\beta_6$	-0.082	[-0.207; 0.055]	-0.049	[-0.182; 0.085]
$\beta_7$	0.083	[-0.091; 0.240]	0.023	[-0.144; 0.189]
$\alpha$	0.244	[ 0.230; 0.260]	0.303	[ 0.280; 0.326]
$\eta$	3.111	[ 2.893; 3.343]	2.844	[ 2.652; 3.052]
$\delta$	0.497	[ 0.485; 0.500]	0.687	[ 0.631; 0.740]